J. Cosmet. Sci., 72, 379–398 (July/August 2021)

Skin Permeation of Hazardous Compounds of Tobacco Smoke in Presence of Antipollution Cosmetics

SORAYA PONTES-LÓPEZ, ANA GONZÁLVEZ, FRANCESC A. ESTEVE-TURRILLAS, AND SERGIO ARMENTA

Department of Analytical Chemistry, University of Valencia, Burjassot 46100, Spain (S.P.-L., F.A.E.-T, S.A.); RNB, Cosmetic Laboratory, Industrial Estate La Pobla L'Eliana, La Pobla de Vallbona 46185, Spain (A.G.)

Accepted for publication May 14, 2021.

Synopsis

Negative health effects of active and passive smokers have been widely described, but the effect of tobacco smoke on the skin has been less explored. In this study, an analytical methodology has been developed to evaluate the dermal permeation of hazardous compounds present in tobacco smoke, using an exposition chamber to simulate finite and infinite smoking conditions, *in vitro* vertical Franz diffusion cells, and Strat-M® membranes as human skin simulants. Moreover, the antipollution effect of three cosmetics has been evaluated, showing a significant efficacy to reduce dermal permeation of hazardous tobacco-smoke compounds such as of nicotine and aromatic hydrocarbons.

INTRODUCTION

Cigarette smoke is a complex mixture, consisting of thousands of compounds, many of which are known carcinogens, cocarcinogens, or tumor promotors (1). It is a dynamic mixture of sidestream and exhaled mainstream smoke resulting from combustion of cigarettes. Health effects of cigarette smoking are well known (2), but smoking effects on skin have been less studied. The presence of free radicals, both in the tar and the gas phase (3,4), converts the smoke into a highly reactive nature with potential damaging effects on the skin surface (5). It is known that cigarette smoking induces premature skin aging (6,7). The relationship between cigarette smoking and skin aging is supported with epidemiological studies and *in vitro* mechanistic evidence (8,9,10). It has been also evidenced that cigarette smoke can be associated with psoriasis (11).

Address all correspondence to Sergio Armenta at sergio.armenta@uv.es

As a result of this concern, different antipollution products have recently irrupted in the cosmetic market (12). As complete avoidance of smoke pollution is impossible in cigarette smokers, antipollution cosmetic products have three main mechanisms of action: i) prevention (film-forming ingredients or skin barriers), ii) protection (antioxidants to neutralize free-radicals), and iii) repair (13). To date, published *in vitro* efficacy methods for antipollution cosmetics are based on the effect of pollutants on the skin structure using human epidermal keratinocytes and reconstructed skin models (14,15), and human fibroblasts (16). Those procedures evaluate modifications suffered by the skin in presence or absence of cosmetic products; however, they do not evaluate dermal absorption of air pollutants through the skin.

In this sense, the Organization for the Cooperation and Economic Development has published a series of guidelines for the *in vivo* (n. 427) and *in vitro* (n. 428) evaluation of dermal absorption of chemicals (17,18). Those procedures are based on the determination of absorption rates by passive diffusion using vertical diffusion cells. Using a similar approach, the dermal exposure of nicotine from liquid solutions (19,20,21), benzene from gasoline (22), and different organic compounds from pure liquids (23) have been evaluated.

The present study is focused on the development of an appropriate analytical methodology for the evaluation of dermal absorption of different organic compounds from cigarette smoke, using *in vitro* vertical Franz diffusion cells and simulant human skin membranes to, on one hand, assess the effectivity of antipollution cosmetic products and, on the other hand, describe and evaluate the dermal absorption process of some well-known organic contaminants from cigarette smoke. In order to do that, a multi-pollutant approach simulating field exposition conditions at finite and infinite doses has been employed.

METHODS AND MATERIALS

REAGENTS AND MATERIALS

Benzene, toluene, ethylbenzene, o-xylene, m-xylene, p-xylene, chlorobenzene, styrene, p-cymene, limonene, naphthalene, acenaphthylene, 1-methylphenanthrene, 2-methylanthracene, and nicotine were provided by Scharlau (Barcelona, Spain) and Sigma-Aldrich (St. Louis, MO). Toluene-d_8 and nicotine-d_4, provided by Sigma-Aldrich, were employed as internal standards. Standards and working solutions were prepared in acetone (GC analysis grade) obtained from Scharlau. Methanol, ammonium acetate, and phosphate saline buffer, obtained from Scharlau, were used for mobile phase composition and LC standards preparation. Strat-M® membranes were purchased from Millipore (Temecula, CA).

American-blend cigarettes, containing approximately 50% Virginia, 37% burley, and 13% oriental varieties, were obtained from local tobacco shops.

COSMETIC PRODUCTS COMPOSITION

Antipollution cosmetic A is a daily skin care cream (viscous emulsion) that protects from sunlight and blue radiation, preventing skin photo-ageing. This cosmetic product firms, smoothes, and reduces wrinkles, due to paracress plant extract. It is suited to sensitive skin because of the presence of active principles such as liquorice extract and bioactive molecules from stem cells from cotton (see Table I).

Table I
Composition of Cosmetic Products Evaluated

	Cosmetic A	Cosmetic B	Cosmetic C
Water (% w/w)	60–65	50–60	70–75
Silicones (% w/w)	3.0	6.8	2.0
Dimethicone	1.0–3.0	5.0–6.0	2.0
Polysilicone	–	0.8	–
Dimethicone-vinyl dimethicone crosspolymer	0.3	–	–
Polymers including surfactants (% w/w)	3.8	6.6	6.3
Acrylates	0.3	0.7	–
Stearates	1.20	4.5	4.0
Carbomers	–	0.15	0.3
Polyisobutene	0.5	0.5	–
Others	1.8	0.75	2.0
Emollients (% w/w)	9.6	12.4	8.4
Ethylhexyl isononanoate	2.0	4.0	–
Dicaprylyl carbonate	–	3.0	4.0
Caprylyl glycol	2.0	0.1–0.3	–
Ethylhexyl olivate	–	2–2.5	–
Olive oil unsaponifiables	–	0.1–0.4	–
Cetearyl alcohol	1.45	–	2.0
Myristyl myristate	–	–	0.5
Collagen	–	–	0.1–0.5
Squalane	2.5	–	–
Palmitic acid	0.5	–	–
Others	1.15	2.64	1.65
Glycerine (% w/w)	5.0–10.0	5.0–10.0	5.0–10.0
UV filters (% w/w)	4.0	10.0	0.0
Ethylhexyl triazone	1.5–3.5	1.5–3.5	–
Butyl methoxydibenzoylmethane	1.5–3.5	2.0–4.0	–
Octocrylene	–	4.0–7.0	–
Fillers (% w/w)	0.5–1.0	1.0	1.0–3.0
Talc	0.4–0.5	1	0
Mica	0.2–0.4	0	0
Silica	0	0	0.4
Silicates	0	0	2.2
Antioxidants (% w/w)	0.7	0.8	0.8
Xanthan gum (% w/w)	0.0005	0.0025	0.014
Others (% w/w)	5.0–6.0		1.0–3.0
	Dunaliella salina extract		*Caesalpina spinosa* fruit extract
	Acmella oleracea extract	1.5–3.0	*Kappaphycus alvarezii* extract
	Gossypium herbaceum callus culture	*Gossypium herbaceum* callus culture	*Lycium barbarum* callus culture extract
	Glycyrrhiza glabra root extract		*Gossypium herbaceum* callus culture

Antipollution cosmetic B is also a rich texture cream (viscous emulsion) that welfares and protects the skin against external agents such as contamination, sun radiation (infrared, UV, and blue light) and antioxidant agents, increasing skin firmness and elasticity while intensely moisturizing. These properties for treating and preventing adverse environmental effects are provided by its combination of active principles including, vitamin C, peptides (carnosine and oligopeptide-1), alantoine, pantenol, and bioactive molecules from stem cells from cotton.

Antipollution cosmetic C is a lifting cream remodelling facial oval (viscous emulsion) that welfares and protects the skin against external agents, increasing skin firmness and elasticity. These properties for treating and preventing adverse environmental effects are provided by its combination of active principles including, hydrolyzed collagen, and bioactive molecules from stem cells from cotton and *Lycium barbarum* and plant and algae extracts including *Caesalpinia spinosa* fruit and *Kappaphycus alvarezii*.

SIMULATION CHAMBER

A specifically modified closed enclosure model HZ08252, with 640 L internal volume, from Bruker (Billerica, MA) was used as simulation chamber (see Figure 1). Clean air was introduced at 2.0 L min^{-1} in the simulation chamber using a MPB1200 rotameter from MPB Industries (Kent, UK), calibrated by a high-volume bubble flowmeter. Two fans with vibration-dampening rubber corners, placed inside the chamber, assured air homogeneity. The simulation chamber was placed in a 50 m^3 closed room, with controlled temperature (25°C ± 1°C) and a fume hood system to avoid operator exposure to hazardous organic compounds from cigarette smoke.

Air monitoring devices were placed inside the simulation chamber to control air quality. An airflow multi-function anemometer TA465-P from TSI (Shoreview, MN), equipped with infrared spectroscopy technology, was used to measure CO_2, CO concentration, temperature, and relative humidity. A CEL-712 Microdust Pro from Casella Cel (Kempston, UK) with a photoelectric sensor was employed to determine the concentration of particulate materials (PM) suspended in air. An Airy Technology P311 (Stoughton, MA) equipped with laser particle counter was used to determine PM in terms of amount of different size particles and a PhoCheck Tiger from Ion Science (Laubach, Germany) to determine VOCs based on the use of a photo-ionization detector. All devices were previously calibrated and employed after stabilization.

SMOKING MACHINE

Smoking machine was built using a Laboports mini diaphragm vacuum pump, from VWR International (Radnor, PA), operating at 5.5 L min^{-1} flow rate. Vacuum pump was connected to three cigarettes using silicone tubing (10 mm internal diameter) and three-way hose fittings (see Figure 1). Inhaled smoke was flowed through a vacuum trap and reintroduced in the chamber. For dermal absorption experiments in finite conditions, the smoking machine was turned on and three cigarettes were simultaneously lighted up. Cigarettes were completely consumed after 10 min, providing a maximum exposure time of 40 min. On the other hand, for dermal absorption experiments in infinite conditions, three cigarettes were simultaneously smoked every 30 min, being 8 h the maximum exposure time.

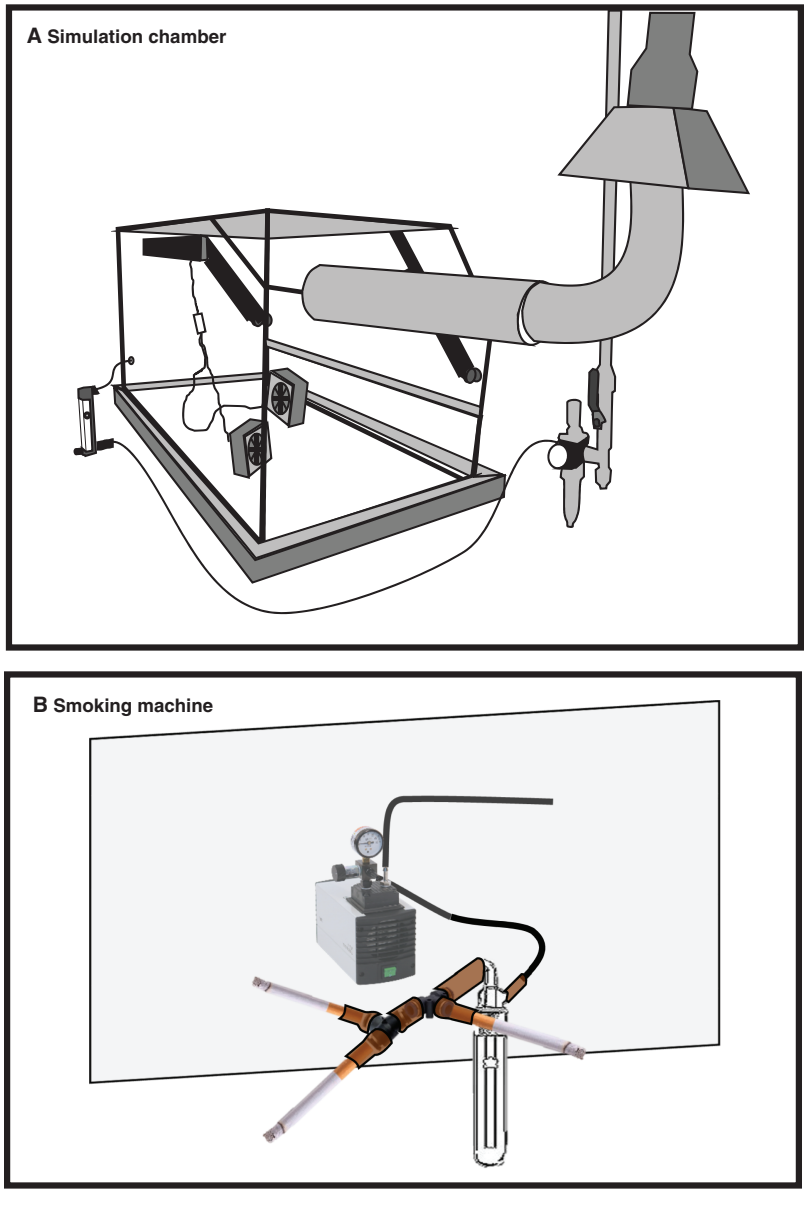

Figure 1. Scheme of (A) the developed exposition chamber and (B) smoking machine used to perform dermal absorption studies of hazardous organic compounds from cigarette smoke.

ABSORPTION STUDIES IN THE SIMULATION CHAMBER

In vitro dermal absorption studies were performed using modified vertical diffusion cells, following the Franz method (24,25). The atmosphere of the simulation chamber acted as donor compartment, while 12 mL saline solution, containing 0.9% (w/v) NaCl and 0.15 M phosphate buffer (pH 7.4), was the receptor solution. Temperature was maintained at 25°C by control of the room temperature. Chamber temperature,

humidity, and PM and VOC concentration inside the simulation chamber were continuously monitored during all the experiments. Receptor solutions were continuously stirred using Teflon-coated magnetic stirrers. Strat-M® membranes (14 mm diameter, being the exposed surface of 0.7 cm^2) were used in the modified vertical diffusion cells as skin simulants (26).

Effectiveness of the antipollution cosmetics was evaluated by homogeneously applying 2 mg product per cm^2 exposed membrane, being this side of the membrane in contact to the contaminated atmosphere. Control experiments were performed with the Strat-M® membrane at the same conditions without cosmetic application. The amount of hazardous organic compounds present in the membrane and receptor solutions were determined after different exposure times.

DETERMINATION OF HAZARDOUS ORGANIC COMPOUNDS FROM CIGARETTES IN THE SIMULATION CHAMBER

The concentration of hazardous organic compounds inside the chamber was measured by active sampling using a low-volume personal air sampling TUFF Standard from Casella measurements (Bedford, UK), operating with a low flow adaptor at a flow rate of 40 mL min^{-1} for 5 min. Glass thermal desorber (TD) tubes, capped with perfluoroalkoxy-polytetrafluoroethylene (PFA-PTFE) ferrules, were obtained from Perkin Elmer (Waltham, MA). TD tubes were filled with 150 mg of Tenax TA (35–60 mesh) provided by Alltech (Selmsdorf, Germany). Tenax was conditioned prior to sampling at 300°C during 2 h.

Active sampling pump flow was regulated using an ADM calibrated flowmeter (Agilent Technologies, Palo Alto, CA) before each sampling. After sampling, tubes were capped with PFA-PTFE ferrules and stored at −20°C until analysis. TD tubes were thermally desorbed using a Turbo Matrix series TD from Perkin Elmer coupled to a Trace GC-Polaris Q gas chromatography-mass spectrometry (GC-MS) detector from Finnigan (Waltham, MA), equipped with an Agilent HP-5MS capillary column (30 m, 0.25 mm, 0.25 μm).

Thermal desorption was carried out at 260°C for 20 min using a 75 mL min^{-1} helium flow rate and desorbed analytes were transferred to a Tenax cold trap at −10°C. A quick trap desorption was carried out at 270°C at 99°C s^{-1} and the analytes were desorbed and directly transferred to the chromatographic column, using a transfer line set at 275°C, with a helium constant flow of 0.8 mL min^{-1} and a split flow of 1:15. GC temperature program was 40°C, held for 8 min, increased at rate of 20°C min^{-1} up to 200°C, and held for 2 min. MS ion source and transfer line temperatures were set at 300°C and 250°C, respectively. Full scan acquisitions were performed using a mass range from 50 to 200 m/z.

Calibration curve was prepared in Tenax packed TD tubes spiked with 10 μL target analytes standard prepared in acetone, with a final added amount from 0.1 to 4.0 μg. Additionally, 10 μL toluene-d_8 internal standard solution (10 mg L^{-1} in acetone) was added inside the Tenax tube. Table II shows m/z ions, retention time, and analytical features of studied compounds.

For the analysis of hazardous organic compounds absorbed in the synthetic membrane, a similar procedure was used introducing in TD tubes 25 mg of Strat-M® membrane. Calibration curves were prepared in TD tubes loaded with 25 mg of Strat-M® membrane and spiked with 10 μL target analytes standard prepared in acetone, with a final added amount from 0.1 to 4.0 μg. Additionally, 10 μL toluene-d_8 internal standard solution (10 mg L^{-1} in acetone) was added.

Table II
Analytical Features, Including Selected Ions and Retention Time, of the Organic Compounds Determined in Cigarette Smoke by Active Sampling and Analyzed by TD-GC-MS and HS-GC-MS

Analyte	Ions (m/z)	Retention time (min)	Lineal range (ng)	LOD[a] (ng)	LOQ[b] (ng)	R^2
Benzene	77, 78	2.50	20–4,000	6	20	0.995
Toluene	91, 106	4.43	20–4,000	6	20	0.998
Chlorobenzene	112	7.63	200–4,000	50	170	0.978
Ethylbenzene	91, 106	8.57	100–4,000	30	100	0.997
m+p-xylene	91, 106	9.27	200–4,000	60	200	0.992
Styrene	116	10.62	500–4,000	150	500	0.984
o-xylene	104	10.65	200–4,000	50	170	0.994
p-Cymene	91, 117	13.40	350–4,000	100	330	0.985
Limonene	67, 93	13.47	200–4,000	60	200	0.999
Naphthalene	128	15.10	20–4,000	5	17	0.994
Nicotine	84, 133	16.30	200–4,000	50	170	0.989
Acenaphthylene	152	17.00	20–4,000	5	17	0.979
2-methylanthracene	192	18.32	100–4,000	25	83	0.996
1-methylphenanthrene	192	19.60	100–4,000	25	83	0.996

[a] Limit of detection
[b] Limit of quantification

HS-GC-MS DETERMINATION

Analysis of hazardous organic compounds in receptor solutions was performed using an Agilent 7697A head space (HS) injector, a 7890A GC, and a 53975C inert XL EI/CI MSD with triple-axis single quadrupole detector. Five milliliter receptor solution and 200 ng mL^{-1} of internal standard (toluene-d_8) were introduced in a 10-mL HS glass vial. HS vial was hermetically closed, heated at 60°C for 20 min, and HS was measured by GC-MS. Injector temperature was 250°C, employing 0.8 mL min^{-1} constant flow helium as carrier gas. Capillary column and GC oven temperature program were that previously described in TD-GC-MS analysis. Electron-impact ionization was performed at 70 eV and MS acquisitions using selected ion monitoring (SIM) mode.

LC-MS-MS

Nicotine determination in receptor solution was performed by LC-MS. An UHPLC-MS instrument model ACQUITY ® TQD, from Waters (Milford, MA), with a KINETEX C18 evo (50 x 2.1 mm, 1.7 µm) column, from Phenomenex (Torrance, CA). Mobile phase consisted of 50 mM ammonium acetate in water (A) and methanol (B). Gradient elution from 5% to 95% mobile phase B in 2 min was used with a flow rate of 0.4 mL min^{-1}, a 5 µL injection volume, and 30°C column temperature.

MS acquisitions were done using 3.5 kV capillary voltage, 120°C source temperature, 300°C desolvation temperature, and 690 L h^{-1} desolvation gas flow rate. Multiple reaction monitoring (MRM) conditions were adjusted for nicotine and nicotine-d_4, being the transitions m/z 163 → 130 and 167 → 136, respectively selected.

RESULTS AND DISCUSSION

IDENTIFICATION OF TOBACCO SMOKE COMPOUNDS INSIDE THE SIMULATION CHAMBER

Cigarette smoke is an aerosol consisting of small, gas-phase-suspended droplets with a complex chemical composition of over 8,700 identified constituents (27), but it has been estimated that the actual number may approach 100,000 (28). A vast amount of literature has appeared since 1950 on tobacco-smoke constituents (29,30,31). Compounds from cigarette smoke can be classified as neutral gases, carbon and nitrogen oxides, amides, imides, lactames, carboxylic acids, lactones, esters, aldehydes, ketones, alcohols, phenols, amines, *N*-nitrosamines, *N*-heterocyclics, aliphatic hydrocarbons, monocyclic and polycyclic aromatic hydrocarbons, nitriles, anhydrides, carbohydrates, ethers, nitro compounds, and metals (32).

The aim of this paper is not to provide a complete list of organic compounds from tobacco smoke but to demonstrate the usefulness of the simulation chamber to generate a polluted atmosphere that represents a situation close to the real one. In this sense, Table III provides a list of the potentially identified organic compounds after active sampling of the simulation chamber air during the simultaneous combustion of three cigarettes using the developed smoking machine. Identification has been done by TD-GC-MS after comparison of the obtained MS spectra with those of National Institute of Standards and Technology (NIST, Gaithersburg, MA) Mass Spectral Library, containing more than 300,000 MS spectra of organic compounds. Moreover, when possible, GC retention time

Table III
Retention Time and Selected Ions of Identified Analytes from Cigarette Smoke Inside the Simulation Chamber

t_R (min)	m/z	Potential analytes
1.61	43	Isoprene
1.95	55, 56	1-nitropentane
2.02	41, 43	Trans cyclopent-1-en-3,5-diol 2-, 3-methylfuran
2.30	77, 78	1,4-cyclohexadien
2.52	77, 78	Benzene
2.82	43, 55	2-methyl-4-pentenal Tetrahidro-4-methyl-3-methylenfuran
2.99	43, 79	5-methyl-1-hexin 4-isopropylcyclohexanol
3.08	95, 98	2,5-dimethylfuran
3.40	65, 66	Phenol
3.76	91	1-(1,3-butadienyl)-2-vinylcyclobutane [(cyclohex-1-en-3-yl)methyl]benzene
3.99	79	Pyridine 5,5'-oxibis[(E)-1,3-pentadiene]
4.21	68	t-butyl acetylene 1S-(-)-N-(cyclopent-2-en-1-yl)hydroxylamine
4.43	91, 92	Toluene
4.61	77	5,5-dimethylcyclopentadiene 1-methylcyclohexa-2,4-diene

(*Continued*)

Table III. (*Continued*)

t_R (min)	m/z	Potential analytes
4.78		2-[(methylsulfonyl)oxy]cyclohexyl methanesulfonate 1-bromo-3,4-dimethyl-2-pentene
5.15	41	(1-allylcyclopropyl)methanol 3,3-dimethyl-1,6-heptadiene 5-nitro-4-nonene
5.50	94, 110	2-isopropyl-furane 3-tert-butyl-1,5-cyclooctadiene
6.52	65,92	3-methylpyridine Aniline
6.84	94	2-dimethylaminopyridine
6.84	94	p-Cresol
7.28	95	Furfural
7.55	77, 112	Chlorobenzene
8.57	91, 106	Ethylbenzene
9.27	91, 106	m-/p-xylene
10.62	78, 104	Styrene
10.65	91, 106	o-xylene
12.55	120	o-/m-/p-ethyltoluene 1,2,3-trimethylbenzene
12.65	104	3-vinylpyridine
12.96	120	Isopropylbenzene 1,2,4-trimethylbenzene o-/m-/p-ethyltoluene
13.01	118	E-1-phenylpropene 2-propenyl-benzene 2,3-dihydro-1H-indene
13.40	91, 117	p-cymene
13.47	67, 93	dl-limonene
15.10	128, 129	Naphthalene
16.30	84, 133	Nicotine
17.00	152, 151	Acenaphthylene
17.55	41	Nonadecane
18.32	192	2-methylanthracene
19.60	192	1-methylphenanthrene
22.82	121	Squalene

of the identified peaks was compared with those of analytical standards prepared for this purpose. As it can be seen, the list includes isoprene, benzene- and aromatic-related compounds, pyridine, aniline, styrene, terpenes, nicotine, and polycyclic aromatic hydrocarbons. From those compounds a selection of 15 compounds, including benzene, toluene, ethylbenzene, and xylenes (BTEX), chlorobenzene, styrene, p-cymene, limonene, naphthalene, nicotine, acenaphthylene, 2-methylanthracene, and 1-methylphenanthrene, were selected as representative compounds for further studies.

DESIGN AND EVALUATION OF THE SIMULATION CHAMBER CONDITIONS

Once representative compounds from cigarette smoke have been selected, the homogeneity of the simulation chamber atmosphere was assessed. In this sense, permeability experiments were carried out using Strat-M® membrane in the modified vertical diffusion

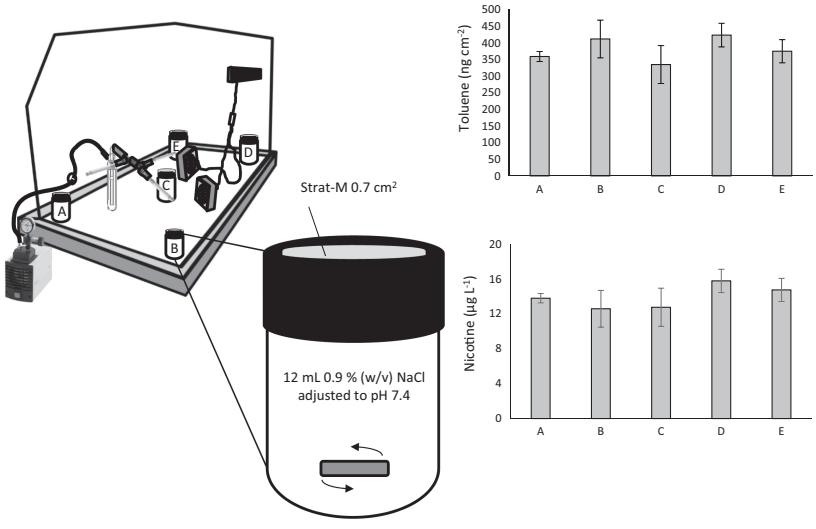

Figure 2. Scheme of the modified vertical Franz diffusion cell and used in this study and results obtained from the five evaluated points inside the simulation chamber to evaluate air homogeneity.

Franz cells placed at different locations inside the chamber (see Figure 2). An average concentration of 380 ± 40 ng cm^{-2} toluene was found in the synthetic membrane, determined by TD-GC-MS; while 13.9 ± 1.3 µg L^{-1} nicotine were found in the receptor solution, determined by LC-MS-MS. The obtained precision was appropriate, established as relative standard deviation (RSD) of five measurements (each corner and the center of the chamber), being lower than 10%. Thus, the placement of two electric fans inside the chamber assured a total homogenization of inner atmosphere, being adequate to perform dermal absorption studies in any position of the simulation chamber.

DERMAL ABSORPTION IN FINITE DOSE CONDITIONS

Finite dose experiment was carried out by the combustion of three cigarettes, which were consumed in approximately 10 min. Several parameters were monitored inside the exposure chamber to evaluate the combustion process during the experiment, giving the next values. Temperature and relative humidity were almost unaffected with average values of 24.8°C ± 0.2°C and 40.1% ± 0.9%, respectively. VOCs, CO, and CO_2 concentration background levels were 101, 0.45, and 1045 mg m^{-3}, respectively, which increase to a maximum around 1200 s (20 min) of 8337, 130, and 3021 mg m^{-3}, respectively, due to the cigarette combustion. With a similar profile, PM concentration background concentration was 0.01 mg m^{-3} that increased till 339 mg m^{-3}. The concentration of target compounds in the chamber air was monitored by active sampling, at 5 min intervals, for a total time of 2 h. Figure 3 shows the concentration of nicotine, toluene, ethylbenzene, and p-cymene in the chamber air, selected as representative compounds. As it can be seen in Figure 3, the concentration profile shows a rapid increase of analyte concentration till a maximum at 15–20 minutes and later, a decrease in concentration at reduced speed. The reached maximum concentration values were 16.58, 3.15, 0.71, and 0.41 mg m^{-3} air for nicotine, toluene, ethylbenzene, and p-cymene, respectively. The average concentration of these compounds in the 0–30-min interval were 9.70, 2.07, 0.26, and 0.41 mg m^{-3}, respectively.

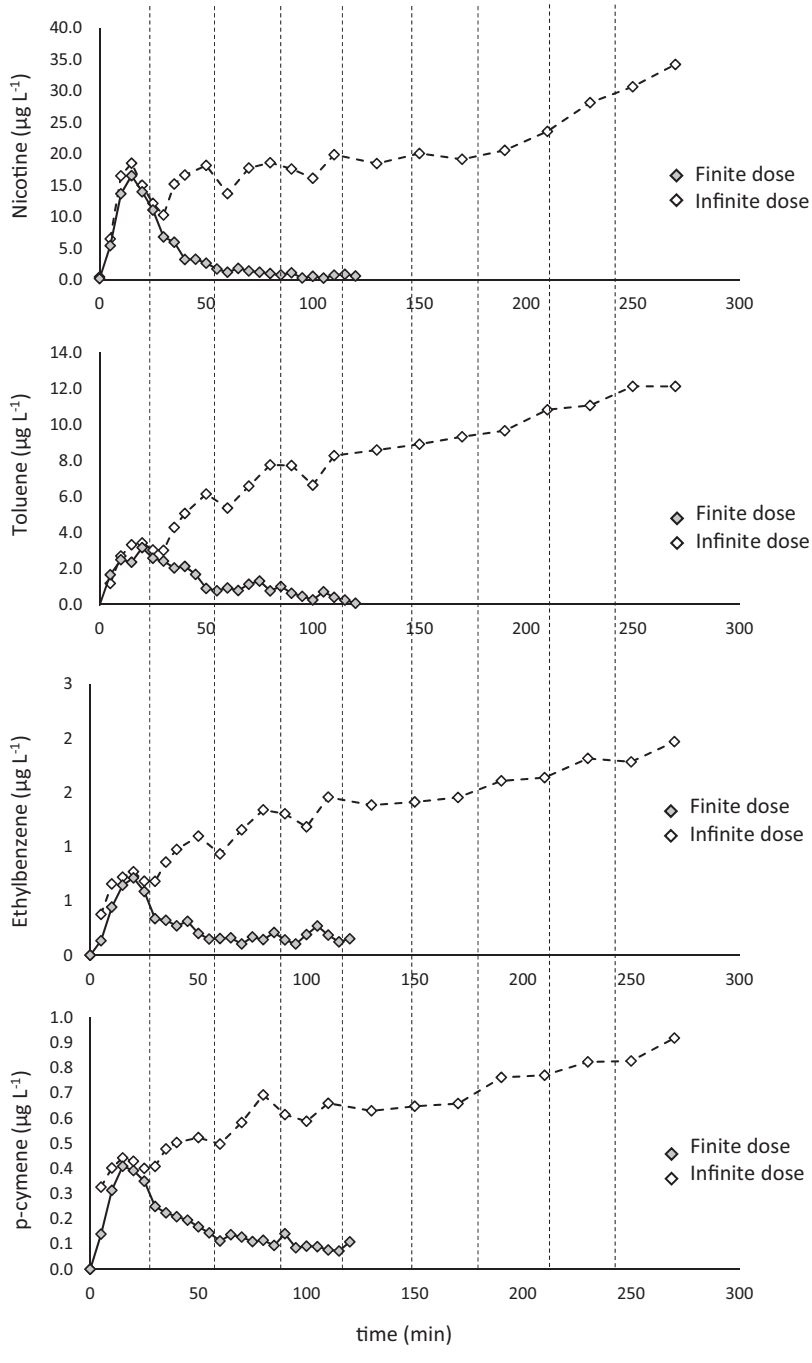

Figure 3. Concentration profile of selected hazardous organic compounds from cigarette smoke inside the simulation chamber measured by active sampling in finite (grey dots) and infinite (white dots) dose conditions.

In vitro dermal absorption studies were performed using finite dose conditions, using control Strat-M® membranes without cosmetic (n=3) and membranes treated with a 2 mg cm^{-2} homogeneous layer of cosmetics A, B, and C (n=3). Modified Franz cells were introduced in the chamber, the three cigarettes were burnt, and the cells remained in the chamber during 135 min. Then, the concentration of target analytes was determined in Strat-M® membrane and receiving solution of each cell. Additionally, a reagent blank was also analyzed to check the absence of contaminations.

The obtained concentrations in control experiments are shown in Figure 4 and Table IV. As it can be seen, nicotine was the only compound detected in the receptor solution, while much more compounds were detected in Strat-M® membrane, such as BTEX, styrene, p-cymene, and limonene.

Nicotine concentration in the receptor solution increased with the time, reaching a maximum concentration value at 30-min exposure time (11.6 μg L^{-1}). Under these conditions, the effect of the evaluated cosmetics after 30-min exposure clearly decreases the nicotine dermal absorption with concentrations of 7.9, 6.6, and 7.5 μg L^{-1} for cosmetics A, B, and C, respectively, indicating an antipollution effect over nicotine absorption (see Table IV).

Analysis of Strat-M® membrane in control studies after 30-min exposure provided concentrations of 90 ng cm^{-2} benzene, 160 ng cm^{-2} toluene, 55 ng cm^{-2} ethylbenzene, 400 ng cm^{-2} m+p-xylene, 120 ng cm^{-2} o-xylene, 160 ng cm^{-2} styrene, 71 ng cm^{-2} p-cymene, 500 ng cm^{-2} limonene, and 2,500 ng cm^{-2} nicotine. In the same way, application of cosmetics A, B, and C provided a significant reduction of the amount of target compounds in the membrane (see Table IV), being the antipollution effect confirmed.

DERMAL ABSORPTION IN INFINITE DOSE CONDITIONS

Antipollution effect of cosmetics was also evaluated at extreme situations, using infinite dose conditions performed by the combustion of three cigarettes every 30 min for a total time of 8 h. Under these conditions, the concentration of cigarette smoke components remain at high concentration levels for a long time (see Figure 3). Active sampling was carried out for a total time of 4.5 h with 20-min intervals, providing an average concentration after 30 min of 20 ± 5, 8 ± 2, 1.4 ± 0.3, and 0.7 ± 0.1 μg L^{-1} air for nicotine, toluene, ethylbenzene, and p-cymene, respectively.

In the same way*, in vitro* dermal absorption studies at infinite dose were performed for control and cosmetics A, B, and C, using modified Franz cells for an exposure time of 0.5, 1, 2, 4, and 8 h. Benzene, toluene, and nicotine were detected after 1-h exposure time in the receptor solution of control tests (see Table V), with concentrations of 3.6, 4.8, and 29.0 μg L^{-1}, which increased to 24, 33, and 1,800 μg L^{-1} after 8 h exposition, respectively. Figure 5A shows the concentration in the receptor solution with time, indicating a linear uptake for nicotine, while benzene and toluene seemed to reach the equilibrium at 8 h. Concentration found in Strat-M® membrane of control experiments showed a linear uptake (see Figure 5B and Table VI) that reached the equilibrium after 4-h exposure, with concentration of 540 ng cm^{-2} toluene, 340 ng cm^{-2} ethylbenzene, 410 ng cm^{-2} p-cymene, and 49,700 ng cm^{-2} nicotine.

Table VI shows the target compound concentration in Strat-M® membranes treated with cosmetics A, B, and C. The effect of the cosmetic layer over Strat-M® membranes was a

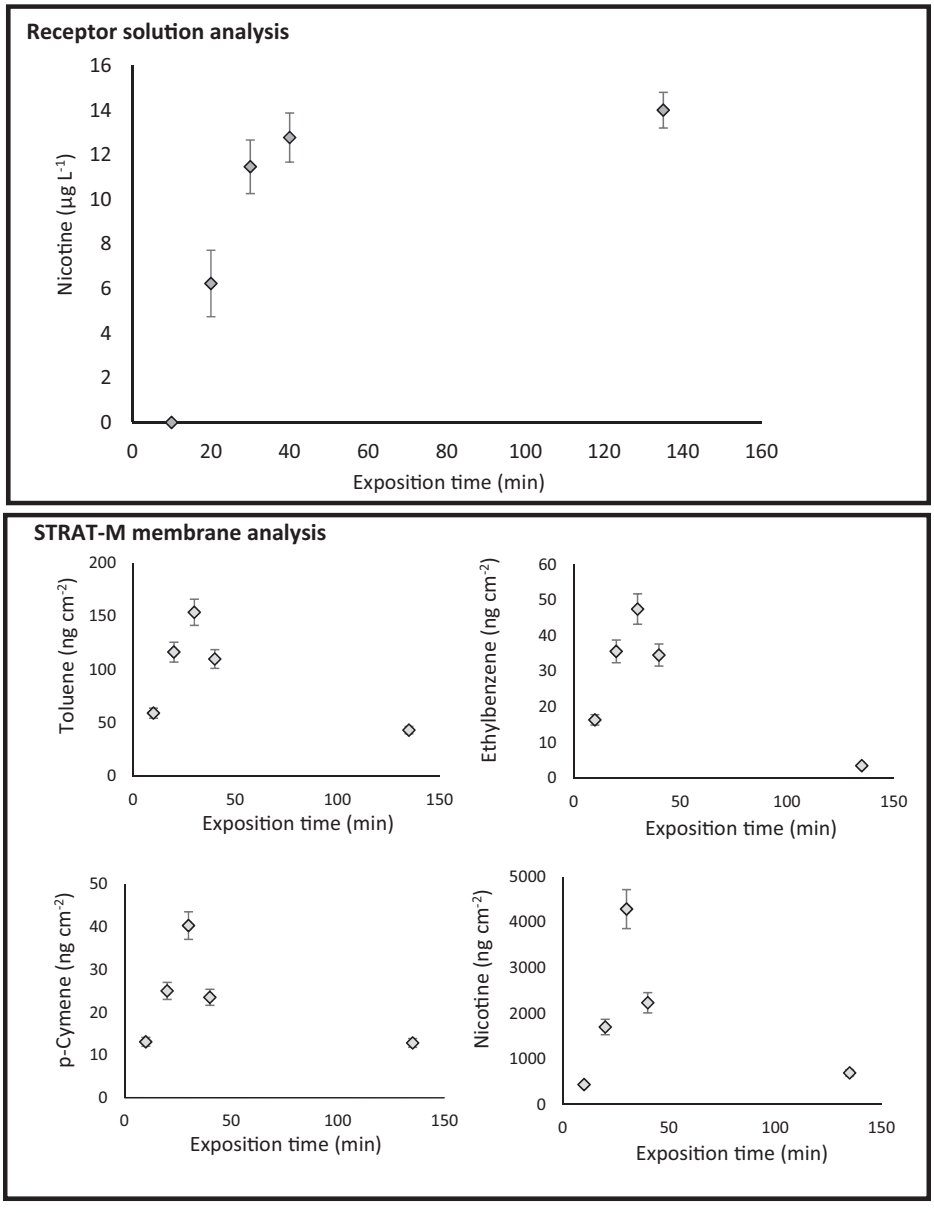

Figure 4. Dermal absorption studies of selected hazardous organic compounds from cigarette smoke in finite dose conditions.

significant reduction of target compounds concentration for short exposition times (1 and 2 h). Nevertheless, the cosmetic effect was reduced with the time, being insignificant for 8 h exposition time.

The antipollution effect of cosmetics A, B, and C at infinite dose has been evaluated by the determination of the concentration of target compounds in the receptor solution. As it can be seen in Tables IV and V, a reduced concentration was observed in cosmetic-treated

Table IV
Concentration of Target Compounds in Strat-M® Membrane and the Receptor Solution after 30 min Exposure at Finite Dose Conditions in Control and Cosmetic Studies

		Concentration (ng cm^{-2} ± s)			
Sample	**Analyte**	**Control**	**Cosmetic A**	**Cosmetic B**	**Cosmetic C**
Strat-M®	Benzene	90 ± 8	50 ± 5	35 ± 4	37 ± 3
	Toluene	160 ± 20	88 ± 9	101 ± 10	65 ± 6
	Ethylbenzene	55 ± 5	40 ± 4	11 ± 2	23 ± 4
	m+p-xylene	400 ± 30	110 ± 10	26 ± 3	46 ± 4
	o-xylene	120 ± 15	54 ± 4	40 ± 3	30 ± 3
	Styrene	160 ± 14	<LOD	<LOD[a]	<LOD
	p-Cymene	71 ± 9	40 ± 3	26 ± 2	10 ± 2
	Limonene	500 ± 50	480 ± 20	143 ± 13	<LOD
	Nicotine	2,500 ± 200	1,600 ± 140	1,400 ± 150	1,400 ± 130
Receptor solution	Nicotine (μg L^{-1})	11.6 ± 1.0	7.9 ± 1.0	6.6 ± 1.1	7.5 ± 1.1

[a] Less than limit of detection

Table V
Concentration of Target Compounds in the Receptor Solution after Different Exposure Times at Infinite Dose Conditions in Control and Cosmetic Studies

		Concentration (μg L^{-1} ± s)			
Exposure time (h)	**Analyte**	**Control**	**Cosmetic A**	**Cosmetic B**	**Cosmetic C**
1	Benzene	3.6 ± 0.4	2.4 ± 0.3	1.08 ± 0.11	1.35 ± 0.18
	Toluene	4.8 ± 0.5	2.5 ± 0.3	<LOD[a]	1.0 ± 0.2
	Nicotine	29 ± 2	25 ± 3	21 ± 1	19 ± 2
2	Benzene	9.9 ± 0.6	4.3 ± 0.5	2.8 ± 0.3	2.8 ± 0.4
	Toluene	13.3 ± 1.2	5.1 ± 0.5	3.3 ± 0.4	3.0 ± 0.2
	Nicotine	169 ± 15	159 ± 14	116 ± 11	129 ± 12
4	Benzene	15.9 ± 1.3	14.3 ± 1.6	6.5 ± 0.4	11.2 ± 1.5
	Toluene	24 ± 3	23 ± 2	13.3 ± 1.1	15.6 ± 1.8
	Nicotine	660 ± 60	660 ± 50	630 ± 50	640 ± 30
8	Benzene	24 ± 2	20 ± 2	13 ± 2	18.6 ± 1.6
	Toluene	33 ± 3	28 ± 3	18 ± 2	23 ± 2
	Nicotine	1,500 ± 200	1,600 ± 140	1,300 ± 120	1,400 ± 150

[a] Less than limit of detection

experiments for 1 and 2 h exposure times. Cosmetic B reduced the concentration in the receptor solution 72% for benzene, 88% for toluene, and 29% nicotine, compared to control experiments. The effect of cosmetic C was similar with a reduced uptake of 67%, 78%, and 29% for benzene, toluene, and nicotine, respectively. While the cosmetic A showed the less antipollution effect with a reduction in the uptake of 45%, 55%, and 10% for benzene, toluene, and nicotine, respectively. However, the antipollution effect of the evaluated cosmetics was clearly reduced at exposure times higher than 4 h in infinite dose study. Nicotine uptake of cosmetic-treated membranes for long exposure times was almost similar to control experiments, indicating a saturation of the cosmetic layer with the pollutant compound. Nevertheless, antipollution effect remained for benzene

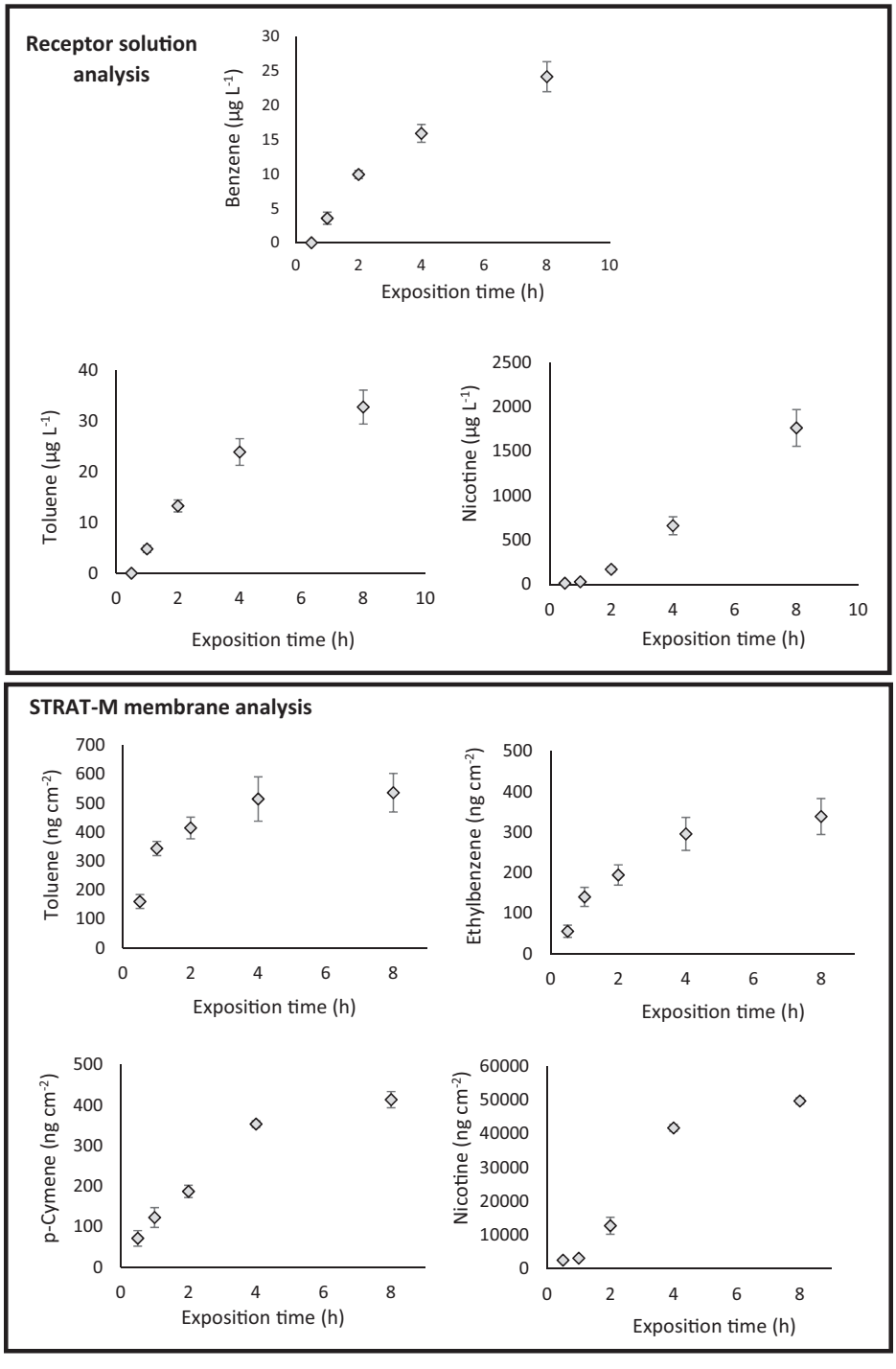

Figure 5. Dermal absorption studies of selected hazardous organic compounds from cigarette smoke in infinite dose conditions.

Table VI
Concentration of Target Compounds in the Strat-M Membrane after Different Exposure Times at Infinite Dose Conditions in Control and Cosmetic Studies

Exposure time (h)	Analyte	Concentration (ng cm^{-2} ± s)			
		Control	Cosmetic A	Cosmetic B	Cosmetic C
1	Benzene	227±9	110±3	93±2	98.3±1.5
	Toluene	343±17	160±8	119±6	127±8
	Ethylbenzene	140±7	54±3	46±3	48±3
	m+p-Xylene	510±30	165±7	158±7	179±9
	o-Xylene	140±7	65±4	54±3	52±3
	Styrene	237±18	86±5	63±4	73±5
	p-Cymene	122±6	68±4	35±2	40±3
	Limonene	760±40	550±30	280±20	310±20
	Nicotine	3,110±160	2,680±70	1,750±60	2,561±70
2	Benzene	332±18	285±18	225±17	253±12
	Toluene	414±15	211±10	142±8	196±8
	Ethylbenzene	194±8	86±7	67±5	75±6
	m+p-Xylene	620±20	285±15	221±12	239±14
	o-Xylene	163±7	87±7	64±5	67±5
	Styrene	299±15	147±9	101±4	98±8
	p-Cymene	187±8	110±8	64±5	60±5
	Limonene	980±50	960±50	510±20	436±18
	Nicotine	12,700±600	12,100±500	13,041±500	9,000±400
4	Benzene	460±20	310±18	285±19	320±20
	Toluene	510±30	247±15	292±18	350±20
	Ethylbenzene	290±20	164±7	157±7	178±7
	m+p-Xylene	950±50	590±30	730±40	560±40
	o-Xylene	230±12	148±6	102±5	178±8
	Styrene	680±50	370±20	390±30	270±20
	p-Cymene	353±18	204±12	168±6	153±6
	Limonene	1600±100	1420±90	1430±110	1130±90
	Nicotine	42,000±2,000	42,000±2,000	41,200±1,800	43,000±2,000
8	Benzene	490±20	480±20	479±18	490±20
	Toluene	540±30	520±20	580±30	517±40
	Ethylbenzene	340±20	311±18	224±15	337±19
	m+p-Xylene	1150±60	1060±50	860±40	1180±50
	o-Xylene	266±15	263±12	196±10	270±20
	Styrene	890±40	750±40	570±30	844±40
	p-Cymene	410±20	302±18	320±16	341±12
	Limonene	2,000±150	1,980±140	1,800±150	1,900±160
	Nicotine	50,000±2,000	50,000±3,000	52,000±2,000	52,000±2,000

and toluene, with a reduced concentration in the received solution of 53% and 45% for cosmetic B, and 26% and 33% for cosmetic C, respectively.

EFFECT OF COSMETICS COMPOSITION ON ANTIPOLLUTION EFFECTIVENESS

Surfactants and barrier-forming polymeric materials have demonstrated an important antipollution effect versus organic compounds (13,33). The concentration of surfactants and polymers, mainly polyacrylates, polystearates, and hydrophobic waxy polymers, in the evaluated antipollution cosmetics was 3.8%, 6.6%, and 6.3% (w/w) for product A, B,

and C, respectively. This difference in the composition of polymers provided significant differences in antipollution effectiveness against organic compounds, being cosmetics B and C, those with higher antipollution effect. Moreover, the percentage of silicones used in the formula, mainly as dimethicone, was also different for the evaluated cosmetics, with concentration values of 3.0%, 6.8%, and 2.0% (w/w) in antipollution cosmetics A, B, and C, respectively. Polydimethylsiloxane has been previously used as synthetic skin simulant in dermal absorption experiments (25), being demonstrated that increasing the width of the polydimethylsiloxane layer decreases flux and increases lag time of organic compounds through the skin. Thus, dimethicone could be responsible of the increase of the antipollution effect at long exposition times.

The addition of high-molecular-weight polysaccharides, such as xanthan gum, an antipollution active principle with demonstrated effects against the adsorption of organic compounds [4], also increases antipollution effectiveness, even at very low concentration. Xanthan gum concentration of cosmetic C was 0.014% (w/w), while for cosmetics A and B was 0.0005% and 0.0025% (w/w), respectively.

Moreover, the presence of mineral particles in antipollution cosmetics, such as talc or silicates, adsorbs organic compounds in its surface (34,35) and, thus, it may improve the antipollution efficiency of cosmetic products. Percentage of fillers such as talc, silica, and silicates in antipollution cosmetic C was higher than that of A and B, which could also explain the increased efficiency of this product compared to A.-

In summary, the high antipollution effect of cosmetic B and C probably should be assigned to synergic effects of polymeric and surfactants, silicones, xanthan gum, and mineral particles, being the combination of all the aforementioned aspects the responsible of an efficient antipollution effect of cosmetic products B and C.

Previous *in vivo* studies, in which a method was developed to demonstrate the effect of antipollution cosmetic products against pollution generated by cigarette smoke included lipid peroxidation in human volunteers (36). The skin of the back of human volunteers is treated with the product under test, exposed to smoke, and then peroxidation of human sebum is assessed. Results confirmed that lipid peroxidation induced in human skin by cigarette smoke could be inhibited by topical antioxidants. Other *in vivo* and *in vitro* studies (37) demonstrated that the application of a face cream formulation containing a film-forming exopolysaccharide prior to exposure to carbon particles significantly decreased particle adherence to skin in human subjects. Moreover, Unilever has recently found that the three main types of film formers, polysaccharide-, acrylate-, and resin-based, enhanced efficacy of cosmetics in preventing lipoperoxidation-based damage to the skin (38).

CONCLUSIONS

A versatile and adaptable analytical methodology has been developed to evaluate the dermal permeation of tobacco-smoke hazardous compounds from contaminated air. Permeation experiments were carried out inside a specifically developed exposition chamber to obtain a representative concentration of tobacco-smoke pollutants. A machine was developed to simultaneously smoke three cigarettes, where inhaled smoke was reintroduced in the chamber. The designed manifold allowed to operate at finite and infinite conditions, with the single combustion of three cigarettes for a short-time exposition (around 40 min) and the combustion of three cigarettes every 30 min for long-time exposition (8 h), respectively.

Permeation of tobacco-smoke pollutants was monitored by control experiment using Franz cells and Strat-M® membranes, being nicotine the major pollutant present in both, Strat-M® membrane and receptor solution, with concentrations of 2.5 μg cm^{-2} and 11.6 μg L^{-1} after a 30-min exposition, respectively. In the case of infinite exposition, nicotine concentration significantly increased to 50 μg cm^{-2} in Strat-M® membranes and 1,500 μg L^{-1} in the receptor solution, after 8 h exposure. The effect of three antipollution cosmetics was demonstrated using the developed conditions, decreasing the permeation of BTEX, styrene, p-Cymene, limonene, and nicotine for exposures of 1 and 2 h. In the case of longer exposure (till 8 h), antipollution effects of the evaluated cosmetics were insignificant, due to a saturation of cosmetic layer over the skin simulant. Thus, antipollution cosmetics should be re-applied from time to time to provide a lasting effect.

ACKNOWLEDGMENTS

We acknowledge the financial support obtained from RNB for the project "Desarrollo de nuevos cosméticos antipolución, urbancream "under the Centro para el Desarrollo Tecnológico Industrial (CDTI) funding project program (CPI-19-027) and that obtained from the Ministerio de Ciencia, Innovación y Universidades, Spain (PID2019-110788GB-I00).

CONFLICT OF INTEREST

The authors declare that they have no known competing financial interests or personal relationships that could have appeared to influence the work reported in this paper.

REFERENCES

(1) International Agency for Research on Cancer, World Health Organization, United Nations, Monographs on the Evaluation of the Carcinogenic Risk of Chemicals to Humans: Tobacco smoke and involuntary smoking, International Agency for Research on Cancer, Lyon (2004). ISBN 92 832 1283 5.
(2) S. K. Das, Harmful health effects of cigarette smoking, *Mol. Cell. Biochem.,* 253, 159–165 (2003).
(3) E. Randerath, D. Mittal, and K. Randerath, Tissue distribution of covalent DNA damage in mice treated dermally with cigarette "tar": Preference for lung and heart DNA, *Carcinogenesis*, 9, 75–80 (1988).
(4) W. A. Pryor, M. Tamura, and D. F. Church, ESR spin trapping study of the radicals produced in NOx/olefin reactions: A mechanism for the production of the apparently long-lived radicals in AS phase cigarette smoke, *J. Am. Chem. Soc*., 106, 5073–5079 (1984).
(5) D. Bernhard, C. Moser, A. Backovic, and G. Wick, Cigarette smoke- an aging accelerator?, *Exp. Gerontol.,* 42(3), 160–165 (2007).
(6) D. P. Kadunce, R. Gress, R. Kanner, J. L. Lyone, and J. Zone, Cigarette smoking: risk factor for premature facial wrinkling, *Ann. Intern. Med.*, 114(10), 840–844 (1991).
(7) R. A. Norman and M. Rappaport, Smoking, Obesity/Nutrition, Sun, and the Skin. in *Preventive Dermatology*, R. A. Norman. Ed. (Springer, London), pp. 17–20(2010). DOI: 10.1007/978-1-84996-021-2_2
(8) D. N. Doshi, K. K. Hanneman, and K. D. Cooper, Smoking and skin aging in identical twins, *Arch. Dermatol*., 143(12), 1543–1546 (2007).
(9) J. S. Koh, H. Kang, S. W. Choi, and H. O. Kim, Cigarette smoking associated with premature facial wrinkling: image analysis of facial skin replicas, *Int. J. Dermatol*., 41(1), 21–27 (2002).

(10) E. Aizen and A. Gilhar, Smoking effect on skin wrinkling in the aged population, *Int. J. Dermatol*., 40(7), 431–433 (2001).
(11) Q. Zhou, U. Mrowietz, and M. Rostami-Yazdi, Oxidative stress in the pathogenesis of psoriasis. *Free Radic. Biol. Med*., 47(7), 891–905 (2009).
(12) C. Juliano and G. A. Magrini, Cosmetic functional ingredients from botanical sources for anti-pollution skincare products, *J. Cosmetics*, 5, 19 (2018).
(13) N. Mistry, Guidelines for formulating anti-pollution products, *J. Cosmetics*, 4, 57 (2017).
(14) J. Soeur, J. P. Belaïdi, C. Chollet, L. Denat, A. Dimitrov, C. Jones, P. Perez, M. Zanini, O. Zobiri, S. Mezzache, D. Erdmann, G. Lereaux, J. Eilstein, and L. Marrot, Photo-pollution stress in skin: traces of pollutants (PAH and particulate matter) impair redox homeostasis in keratinocytes exposed to UVA1, *J. Dermatol. Sci*., 86, 162–169 (2017).
(15) J. Cotovio, L. Onno, P. Justine, S. Lamure, and P. Catrouxet, Generation of oxidative stress in human cutaneous models following in vitro ozone exposure, *Toxicol. In Vitro*, 15, 357–362 (2001).
(16) Y. Qiao, Q. Li, H.Y. Du, Q.W. Wang, Y. Huang, and W. Liu, Airborne polycyclic aromatic hydrocarbons trigger human skin cells aging through aryl hydrocarbon receptor, *Biochem. Biophys. Res. Commun*., 488, 445–452 (2017).
(17) Organisation for Economic Co-operation and Development, Guidelines for the Testing of Chemicals, Section 4, Test No. 428: Skin Absorption: In Vitro Method, 2004, accessed April 1, 2021, https://doi.org/10.1787/20745788.
(18) Organisation for Economic Co-operation and Development, Guidelines for the Testing of Chemicals, Section 4, Test No. 427: Skin Absorption: In Vivo Method, 2004, accessed April 1, 2021, https://doi.org/10.1787/20745788.
(19) H. F. Frasch and A. M. Barbero, In vitro human epidermal permeation of nicotine from electronic cigarette refill liquids and implications for dermal exposure assessment, *J. Expo. Sci. Environ. Epidemiol*., 27(6), 618–624 (2017).
(20) S. Zorin, F. Kuylenstierna, and H. Thulin, In vitro test of nicotine's permeability through human skin. Risk evaluation and safety aspects, *Ann. Occup. Hyg.*, 43, 405–413 (1999).
(21) B. J Aungst, Nicotine skin penetration characteristics using aqueous and non-aqueous vehicles, anionic polymers, and silicone matrices, *Drug. Dev. Ind. Pharm.,* 14, 1481–1494 (1998).
(22) H. F. Frasch and A. M. Barbero, In vitro human skin permeation of benzene in gasoline: Effects of concentration, multiple dosing and skin preparation, *J. Expo. Sci. Environ. Epidemiol*., 28(2), 193–201 (2018).
(23) L. Schenk, M. Rauma, M. N. Fransson, and G. Johanson, Percutaneous absorption of thirty-eight organic solvents in vitro using pig skin, *PLOS ONE*, 13(10), e0205458 (2018).
(24) S. Pontes-López, J. Moreno, F. A. Esteve-Turrillas, and S. Armenta, Development of a simulation chamber for the evaluation of dermal absorption of volatile organic compounds, *Atmos. Pollut. Res*., 11, 1009–1017 (2020).
(25) S. Pontes-López, J. Moreno, F. A. Esteve-Turrillas, and S. Armenta, Development of a simulation chamber for the evaluation of dermal absorption of volatile organic compounds, *Atmos. Pollut. Res*., 11, 1009–1017 (2020).
(26) A. Haq, B. Goodyear, D. Ameen, V. Joshi, and B. Michniak-Kohn, Strat-M® synthetic membrane: Permeability comparison to human cadaver skin, *Int. J. Pharm*., 547, 432–437 (2018).
(27) A. Rodgman and T. A. *Perfetti, The Chemical Components of Tobacco and Tobacco Smoke, 2nd Ed.*, (CRC Press, Taylor & Francis Group, Boca Raton, FL), p. 1473, (2013).
(28) A. Rodgman, C. J. Smith, and T. Perfetti, The composition of cigarette smoke: a retrospective, with emphasis on polycyclic components, *Hum. Exp. Toxicol.,* 19(10), 573–595 (2000).
(29) J. M. Daisey, K. R. R. Mahanama, and A. T. Hodgson, Toxic volatile organic compounds in simulated environmental tobacco smoke: emission factors for exposure assessment, *J. Exp. Anal. Environ. Epidemiol.,* 8(3), 313–334, (1994).
(30) S. Fischer, B. Spiegelhalder, J. Eisenbarth, and R. Preussman, Investigations on the origin of tobacco-specific nitrosamines in mainstream smoke of cigarettes, *Carcinogenesis*, 11(5), 723–730, (1990).
(31) G. Lofroth and Y. Zebuhr, Polychlorinated dibenzo-p-dioxins (PCDDs) and Dibenzofurans (PCDFs) in mainstream and sidestream cigarette smoke, *Bull. Environ. Contam. Toxicol*., 48, 789–794 (1992).
(32) C. Baumung, J. Rehm, H. Franke, and D. W. Lachenmeier, Comparative risk assessment of tobacco smoke constituents using the margin of exposure approach: the neglected contribution of nicotine, *Sci. Rep.,* 6, 35577 (2016).

(33) S. Pontes-López, A. Gonzálvez, F. A. Esteve-Turrillas, and S. Armenta, Skin penetration of hazardous air pollutants in presence of antipollution cosmetics, *J. Cosmet. Sci*., 72, 33–45, (2021).
(34) H. Hashizume, Adsorption of aromatic compounds in water by talc, *Clay Sci.*, 14, 61–64 (2009).
(35) Y. Lu, Y. Li, D. Liu, Y. Ning, S. Yang, and Z. Yang, Adsorption of benzene vapor on natural silicate clay minerals under different moisture contents and binary mineral mixtures, *Colloids Surf. A Physicochem. Eng. Asp*., 585, 124072 (2020).
(36) S. Bielfeldt, A. Boehling, G. Springmann, K. Wilhelm, Pollution protection and the skin—testing strategies. *Househ. Pers. Care Today*, 11, 81–84 (2016).
(37) M. Narda, G. Bauza, P. Valderas, C. Granger, Protective effects of a novel facial cream against environmental pollution: in vivo and in vitro assessment, *Clin. Cosmet. Investig. Dermatol*., 11, 571–578 (2018).
(38) R. K. Bhogal, S. Gosh Dastidar, D. J. Messenger, J. Muscat, and C. Yuan, WIPO International Patent No. WO/2020/058155, Prevention of pollution damage to the skin of an individual" Inventor: Unilever PLC (2020).